energies

MDPI

Article

Wind Technologies for Wake Effect Performance in Windfarm Layout Based on Population-Based Optimization Algorithm

Yi-Zeng Hsieh [1,2,3], Shih-Syun Lin [4], En-Yu Chang [1], Kwong-Kau Tiong [1], Shih-Wei Tan [1], Chiou-Yi Hor [5], Shyi-Chy Cheng [4], Yu-Shiuan Tsai [4,*] and Chao-Rong Chen [6,*]

1 Department of Electrical Engineering, National Taiwan Ocean University, Keelung City 202301, Taiwan; yzhsieh@mail.ntou.edu.tw (Y.-Z.H.); qwe0912881595@gmail.com (E.-Y.C.); b0114@mail.ntou.edu.tw (K.-K.T.); tanshwei@mail.ntou.edu.tw (S.-W.T.)
2 Center of Excellence for Ocean Engineering, National Taiwan Ocean University, Keelung City 202301, Taiwan
3 Institute of Food Safety and Risk Management, National Taiwan Ocean University, Keelung City 202301, Taiwan
4 Department of Computer Science and Engineering, National Taiwan Ocean University, Keelung City 202301, Taiwan; linss@mail.ntou.edu.tw (S.-S.L.); csc@mail.ntou.edu.tw (S.-C.C.)
5 Green Energy and System Integration R&D Department, China Steel Corporation, Kaohsiung 81233, Taiwan; 147595@mail.csc.com.tw
6 Department of Electrical Engineering, National Taipei University of Technology, Taipei 10608, Taiwan
* Correspondence: ystsai@email.ntou.edu.tw (Y.-S.T.); crchen@ntut.edu.tw (C.-R.C.)

check for updates

Citation: Hsieh, Y.-Z.; Lin, S.-S.; Chang, E.-Y.; Tiong, K.-K.; Tan, S.-W.; Hor, C.-Y.; Cheng, S.-C.; Tsai, Y.-S.; Chen, C.-R. Wind Technologies for Wake Effect Performance in Windfarm Layout Based on Population-Based Optimization Algorithm. *Energies* **2021**, *14*, 4125. https://doi.org/10.3390/en14144125

Academic Editors: Georg Stadtmann, Carsten Croonenbroeck and Davide Astolfi

Received: 18 May 2021
Accepted: 29 June 2021
Published: 8 July 2021

Abstract: The focus of this study is under the auspices of China Steel Corporation, Taiwan, in carrying out the national energy policy of 2025 Non-Nuclear Home. Under this policy, an estimated 600 offshore wind turbines will be installed by 2025. In order to carry out the wind energy project effectively, a preliminary study must be conducted. In this article, we investigated the influence of the wake effect on the efficiency of the turbines' layout in a windfarm. A distributed genetic algorithm is deployed to study the wind turbines' layout in order to alleviate the detrimental wake effect. In the current stage of this research, the historical weather data of weather stations near the site of the 29th windfarm, Taiwan, were collected by Academia Sinica. Our wake effect resilient optimized windfarm showed superior performance over that of the conventional windfarm. Additionally, an operation cost minimization process is also demonstrated and implemented using an ant colony optimization algorithm to optimize the total length of the power-carrying interconnecting cables for the turbines inside the optimized windfarm.

Keywords: wake effects; optimization algorithm; turbines layout; wind distribution

1. Introduction

In recent years, with the rapid development of industries and consumer products, the inadequacy of available steady energy supplies has become increasingly serious, and countries with abundant wind resources have begun to devote much effort to exploit this new source of renewable energy. The use of wind power is also a viable option as a source of clean energy. The fact that the wind velocity at sea is higher than that on land, giving rise to higher power generation for offshore wind turbines. Consequently, there are more and more offshore wind turbines brought into service. These constructions will be fully connected to the power grid in the foreseeable future. After all the installations are completed, the maximum offshore capacity in Europe will rise to 200 GW. Presently, Taiwan's energy goal is to achieve the target of "2025 Non-Nuclear Home". Under this time frame, renewable wind energy power generation should achieve a capacity of 120% of the current output by 2025. Taiwan energy goal is to install 600 offshore wind turbines in total by 2025. However, in addition to the challenge of turbines size and scale, it is also necessary to take all kinds of weather and climate conditions in and around the intended windfarm site into consideration before implementation. Besides, the literature [1] pointed out that in the design stage of a windfarm, if the designers can reduce the wake effect loss, the overall growth rate of the potential output power of a windfarm will improve considerably. However, in the conventional turbines arrangement, the wake effect is often ignored in the study of windfarm efficiency. Therefore, this research focused on rearranging the wind turbines' layout to mitigate the impact of the wake effect.

Over the years, the various literature [2–8] had devoted much effort to the study of windfarm optimization. Among them, [2] evaluated time series models for predicting the power of a windfarm at different time scales, while [3] proposed a Particle Swarm Optimization (PSO) scheme for windfarm optimization. An optimal function-provided scheme and corresponding control strategies were adopted by [4] for a utility-scale energy storage system ESS configured in the windfarm. The authors of [5] presented a data protocol for storing the information for the planning of windfarms. A cost-effective and reliable method to estimate wind fields through deep learning algorithms was also proposed by [6]. A study on the scientific merits of deep learning theory on wind power prediction was conducted and presented in [7]. The authors of Ref. [8] adopted a wind power prediction model based on the deep learning method. Nevertheless, most published works were not based on the actual weather data of a planned windfarm.

In this study, we collected historical weather data provided by Academia Sinica from weather stations near the planned No. 29 windfarm. In addition to analyzing the availability of the original raw data of each weather station, we also added simulated weather data as a large data set to provide data diversity and reliability. Artificial intelligence algorithms were used to suggest an optimal turbines layout, mitigate the wake effect, and enhance the efficiency of the windfarm. Based on the obtained optimal layout of windfarm turbines, an artificial intelligence algorithm was subsequently proposed to provide a set of optimal cable layout plans for the wind turbines. Through this research, we hoped to provide personnel with a reference for planning and methods for optimizing the layout for turbines and connecting cables.

Gu and Li et al. [9] proposed several influencing factors for the layout of windfarms, such as topography, landform, wakes and windfarm wind resources, and other economic characteristics. By analyzing these influencing factors, reference [9] proposed a layout optimization model to achieve the economic benefits of the maximum power generation of a windfarm. Zhao et al. [10] used the advantages of genetic algorithm (GA) technology to solve the multivariable and linear optimization problems and applied it to the optimal design of windfarm electrical systems. The genetic algorithm is adopted to solve the problem in different applications, including the windfarm layout design and evaluation of offshore wind power applications.

The important factors of the objective function optimization are mainly based on the average investment cost and stability. The investment cost includes power generation, loss, general operation, maintenance costs, and final dismantling costs, etc. The genetic algorithm is composed of encoding, decoding, random generation, copying, mating, mutation, parameter adjustments, and other genetic algorithm operations to obtain the best solution [10].

Huang [11] proposed a distributed genetic algorithm (DGA) to find the optimal number and location of wind turbines in large windfarms aiming at maximizing the annual profit. Traditional genetic algorithms (GA) are time-consuming, and is prone to early convergence, and may not always find a global solution. In order to reduce the time needed to find the best solution in a large search space and increase the accuracy of the results obtained, the distributed algorithm is adopted in our current research endeavor. The process involves partitioning a large search space into numerous smaller search spaces and occasionally exchanges some individuals during the evolution process. In this method, a large amount of data is without consideration, thus allowing it to obtain the best solution [11,12].

In the windfarm layout, Ref. [11] proposed GA optimization to solve the wake effect in windfarm and Ant Colony Optimization (ACO) optimization to solve the cable layout problem. Our work adopted the DGA and ACO optimization methodologies. Through the study, we hope to provide the most suitable plan for optimizing the wind turbines' layout in the proposed Taiwan No. 29 windfarm.

Our article was organized as follows. The first section is on the introduction and reviews of the related works. The second section proposes the wind effect and cable layout algorithm. The third section analyzed the results from the windfarm dataset. The last section provides a conclusion on some of the important results of our present study.

2. The Proposed Method

2.1. Wind Energy Momentum Theory and Wake Effect

According to the wind turbine principle [11], wind power is generated by wind energy-driven moving blades that drive a rotor. A spindle produces mechanical energy, with the rotor shaft driving a generator to create electrical energy. In general, wind power efficiency also depends on the methods of power conversion and also on the grid connection. However, our current focus is directed toward the wind effect problem, namely, the wake effect.

Momentum theory:

Momentum theory can be used to describe the relationship between the force acting on the wind rotor and the incoming wind flow and then to calculate the mechanical energy. The following turbines issues are assumed to be in an ideal state, without regard to the wind turbine wake rotation [11,13,14]:

(1) The wind flow is an incompressible uniform fixed-length flow;
(2) The wind rotor is simplified into an actuation disc;
(3) There is no friction on the actuation disc;
(4) There is a wind flow static pressure box at the front and rear of the wind rotor;
(5) The axial force (thrust) is evenly distributed along the actuation disc.

In this research, the following mathematical equations were used to optimize the calculation of the windfarm [11].

The energy power P absorbed by the wind rotor can be expressed as:

$$P = 2\rho A U_1^3 a(1-a)^2 \tag{1}$$

$$a = 0.5(1 - U_4/U_1) \tag{2}$$

$\rho = 1.225$ kg/m^3 is the air density;
U_1 is the wind velocity in front of turbine;
U_4 is the wind velocity behind the turbine;
A is the turbines cover area (m^2).
Turbines power factor C_p is defined as:

$$C_p = 2P/\rho A U_1^3 = 4a(1-a)^2 \tag{3}$$

Wake effect:

In addition to the wind velocity, the effective kinetic energy of the wind is also determined by the wind flow direction of the wind relative to the turbines and the ensuing wake effect [15]. It is assumed that the wind velocity in the windfarm is the same. However, because the upper stream turbines are built in a different position, the wake effect impact will also be caused by a different turbine layout, resulting in a difference in the actual wind velocity as experienced by each turbine [16,17].

According to Katic's derivation model [18], the wake effect will gradually expand as the distance between the two wind turbines increases, but the intensity of the impact will gradually decrease.

Wind velocity difference due to wake effect is derived to be Δv [11]:

$$\Delta v = U_F\left(1 - \sqrt{1 - C_t}\right)\left(\frac{D}{D + 2kX}\right)^2 \frac{A_{op}}{A_b} \tag{4}$$

U_F is the upstream turbines velocity;
C_t is the thrust coefficient;
D is the turbines blade diameter;
k is the wake decay constant;
X is the distance between two turbines;
A_{op} is the overlap area between two turbines;
A_b is the area of the downstream turbines swept by the rotor.

2.2. Application of Genetic Algorithm to Windfarm Layout

A conventional layout of a windfarm will bring about serious wake effects [19] and may result in severe deterioration of the overall operational efficiency of the windfarm. If appropriate mitigation measures can be implemented to alleviate the detrimental wake effect, considerable potential growth in the wind power industry can be realized. Therefore, how to optimize the layout of a windfarm is a major issue for offshore wind power generation.

In this research, the optimizing architecture adopted the genetic algorithm, which takes into consideration the relevant windfarm data and related wind turbine parameters. The best solution was obtained through the encoding, decoding, random generation, replication, mutation, and deployment parameters.

The genetic algorithm is mainly inspired by Darwin's evolutionary theory. Natural selection and survival of the strongest are the laws of evolutionary theory; it simulates the genes, selection, mating, and mutation capabilities of organisms and generates better future generations. Therefore, the optimization problem is transformed into the chromosome gene type by creating the number of chromosomes and then performing the selection and mutation process to find the optimal solution.

Encoding and decoding:

This study deployed the binary encoding method used in genetic algorithms and used the combination of 1 and 0 to represent the characteristics of the chromosome. The chromosome string was assumed to be a windfarm area in the form of an 8 × 8 matrix. The number of wind turbines was fixed at 32 units, and there was one offshore substation. Therefore, the chromosome is 32 turbines which constituted of an 8 × 8 random matrix. The horizontal and vertical spacing were both five times the diameter of the wind turbine blades. For illustration purposes, the random positioning of seven turbines inside a 6 × 6 matrix is depicted in Figure 1.

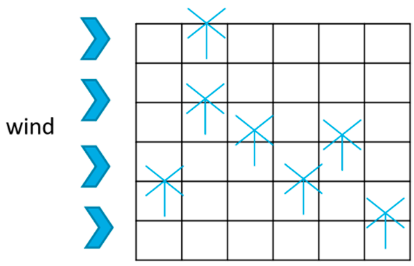

Figure 1. The example for random positioning of 7 turbines in 6 × 6 matrix.

Random matrix generation:

The algorithm of the gene of chromosome string constraints was generated by setting the number of chromosomes to be 200. The program produces five hundred 8 × 8 matrices, with each individual matrix containing 32 randomly built turbines.

Fitness value calculation:

The fitness value is also called the target value and is mainly used to evaluate the quality of each pair of chromosomes during the evolution of each generation. The higher the fitness value, the better the chromosomes can fit the environment. In this system, for example, to build the windfarm in a limited area with a fixed turbines number should predict the best-targeted power efficiency in the windfarm. Equation (5) gives the total power for an individual windfarm through summation of each wind turbine power generation.

$$P_{wf} = \sum_{i=1}^{NT} P_i \tag{5}$$

Among them, P_i is the individual power generation, P_{wf} is the total power generation of all wind turbines in the windfarm, and NT is the number of wind turbines in the windfarm. The wind efficiency (WE) [11] of the windfarm is given as:

$$WE = \frac{P_{wf}}{P \times NT} \tag{6}$$

where P is the rated capacity of a single wind turbine, and higher WE represents better fitness.

Replication:

The replication method is dependent on the size of the chromosome gene, and it can be determined as the next generation in the copied process. The higher adaptation will be the next generation of a large amount of replication, and the lower the degree of adaptation is liable to be eliminated. The process of copying is usually based on a roulette method.

The main function of the roulette-type method is to retain the chromosomes with good fitness value and discard the rest, as shown in Figure 2. Its screening method is based on the probability mode. When the fitness value is better, the probability is higher, and the easier it is for a chromosome to be screened and retained; otherwise, it will be eliminated.

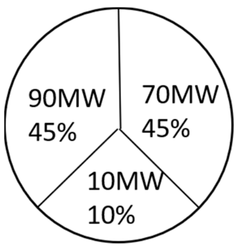

Figure 2. Schematic view of the roulette method.

Crossover:

The mechanism of the crossover step is the focus of the entire in-depth genetic algorithm. Its function is to mate the copied chromosomes in pairs. After the copy is completed, it is sent to the mating pool for the mating process. The mating process consists of randomly selecting two strings (called the mother generation at this time) and exchanging genes (bit data) with each other to form a new string. This new mechanism is also added to the chromosome in relatively large numbers, and thus it can provide superior offspring. This research used the single-point mating method [11].

According to GA optimization, not every chromosome undergoes crossover. The needs according to a preset mating rate (crossover rate) determine the occurrence of the mating parameter as 0.8. In this study, the number of windfarms to be mated is $5 \times 0.8 = 4$. The random selection from the windfarms for single-point mating is adopted. If the chromosome is not undergoing crossover, it will directly be assigned as a next-generation chromosome.

Mutation:

The mutation is mainly used to avoid local optimum. The use of mutation can provide a chance to jump out of the local solution. However, the mutation rate must not be set too high; otherwise, the system will not be able to converge quickly. In this study, the mutation rate was found to be 0.08 for the best conversion of the algorithm. The mutation number of turbines was therefore calculated as $32 \times 0.08 = 2.56$ (which was rounded to 3), and there were three turbines changing their positions. Subsequently, three initially vacant sites within the windfarm were randomly selected to exchange with the three mutated turbines. Figure 3 shows a schematic diagram of the mutation process.

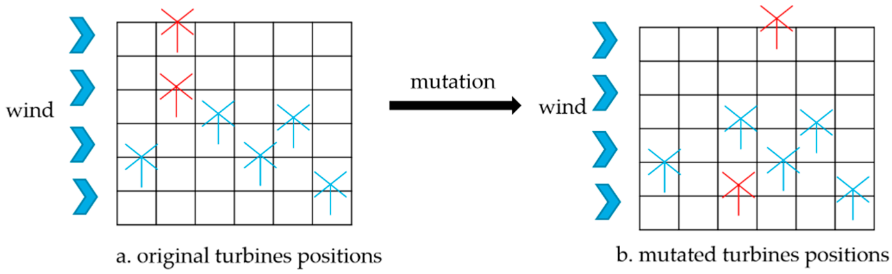

Figure 3. Schematic diagram of the mutations in a 6 × 6 matrix.

The best solution:

Each generation has a contemporary optimal solution, and the optimal solution will be the next generation if the next generation of the optimal solution is better than the best previous generation. A replacement process will then be executed to attain a new best solution. The previous generation will continue to retain the best solution until the end of all generations. The best solution is the global best solution. In this study, the process evolved in such a way as to keep the best solution in the hopes of finding the best placement for wind turbine construction.

2.3. Ant Colony Optimization (ACO) in Turbines Layout

In the natural environment, it is common for a group of ants to carry food on a path and then return to the nest by the same path. This shows that the ants can find the shortest path from the nest to the food source, and they are passing through a path with residual secretions called pheromones. The pheromone concentration will increase in proportion to the number of ants going through the path. Higher pheromone concentration means a higher probability for the ant to follow the path.

Path selection:

The roulette method is used to determine the path [11], and the rule is given by Equation (7):

$$P_{ij}^{k}(t) = \frac{[\tau_{ij}(t)]^{\alpha} \times [\eta_{ij}(t)]^{\beta}}{\Sigma_{s \in a_k} [\tau_{ij}(t)]^{\alpha} \times [\eta_{ij}(t)]^{\beta}} \tag{7}$$

$P_{ij}^{k}(t)$: the probability of ant k moving from turbine i to turbine j;
τ_{ij}: the pheromone concentration between turbine i and turbine j;
η_{ij}: the reciprocal distance between turbines i and turbines j;
$\alpha\beta$: the weight of the pheromone and the distance;
t is the time.

Instant update:

When each ant chooses the path that it is about to walk, a pheromone update is performed on the path. The main purpose of this rule is to avoid producing an overly "strong" path, which may attract all the ants to choose this path, and thus hinder the finding of the optimal solution of the trapped area. In this study, the update rule [11] was as given by Equation (8):

$$\tau_{ij}(\text{new}) = (1 - \rho) \times \tau_{ij}(\text{old}) + (\rho \times \tau_0) \tag{8}$$

ρ: pheromone evaporation parameters, in which $0 < \rho < 1$;
τ_0: path ij is the best path solution.

Offline update:

After completing iterations, the shortest path is updated by a pheromone. For this purpose, the optimal solution is compared to other contemporary feasible solutions, which is an update rule according to Equation (9) [11]:

$$\tau_{ij}(\text{new}) = (1 - \sigma) \times \tau_{ij}(\text{old}) + \rho \times \Sigma_{k=1}^{m} \Delta\tau_{ij}^{k} \quad (9)$$

ρ: pheromone evaporation parameters, in which $0 < \rho < 1$;

$\Delta\tau_{ij}^{k}$: initial pheromone concentration.

The best solution:

The optimal purpose was to find the shortest path to reach a destination, so the ACO's best solution is cable layout length in the windfarm. The following requirements must be met in the selection of the best solution for each generation:

(1) Each turbine must be selected;
(2) Each turbine cannot be selected repeatedly;
(3) If the number of turbines is divisible by the upper limit of the cable carrying number, the remaining unselected turbines will connect to each other.

Punishment mechanism:

If the turbines chosen by the ant overlaps with the best path of the current generation, the pheromone concentration will be slightly reduced, and future generations of ants will have a greater chance to choose other paths.

In this study, in order to meet the needs of the site, the limit for a single cable to withstand the wind turbine was changed to eight wind turbines. After the algorithm was executed, four wind turbine units (eight wind turbines in each group) were obtained according to the results, and all of the assigned wind turbines were respectively connected to the substation locations of each group, which were located at the center points of the four groups. These four substations were finally connected to the shore terminal. Therefore, the selection of the best solution for each generation to meet the requirements was changed to the following four points:

(1) Each ant must go through eight wind turbines;
(2) Each turbine must be selected;
(3) Each turbine cannot be selected repeatedly;
(4) The center point of the wind turbine group selected by the ant colony is set as the location of the substation.

The location of the substation was changed to the location of the relevant substation provided by China Steel Corporation, Taiwan, and four coordinates were assigned to the four actual substation locations. Consequently, the selection of the best solution for each generation is required to meet the following four points:

(1) Each ant must go through eight wind turbines;
(2) Each turbine must be selected;
(3) Each turbine cannot be selected repeatedly;
(4) The wind turbine group selected by the ant colony will form a loop near the location of the substation.

3. Experiments and Results

Turbines module:

In this study, the wind turbine was an Enercon E-101 3 MW synchronous generator module [20]. This type of wind turbine omits the variable speed gearbox and connects the blade drum directly to the generator rotor, thus following the Direct Drive Synchronous Generator (DDSG) model. This study mainly used the unit parameters and Table 1 by [11,20]. The turbines power parameters are shown in Table 2.

Table 1. Enercon E-101 3 MW unit parameters developed from [11,20].

Turbine Model	Enercon E-101 3.05 MW
Number of blades	3
Rated Capacity	3050 kW
Rotor diameter	101 m
Height of hub	99 m
Wind rotor swept area	8012 m^2
C_t	Wind thrust coefficient
C_p	Wind power coefficient

Table 2. Enercon 3 MW E-101 developed from [20].

Wind Velocity (m/s)	Power (KW)	Power Coefficient	Wind Velocity (m/s)	Power (KW)	Power Coefficient
1	0.0	0.000	14	3050	0.227
2	3.0	0.076	15	3050	0.184
3	37.0	0.279	16	3050	0.152
4	118.0	0.376	17	3050	0.127
5	258.0	0.421	18	3050	0.107
6	479.0	0.452	19	3050	0.091
7	790.0	0.469	20	3050	0.078
8	1200.0	0.478	21	3050	0.067
9	1710.0	0.478	22	3050	0.058
10	2340.0	0.477	23	3050	0.051
11	2867.0	0.439	24	3050	0.045
12	3034.0	0.358	25	3050	0.040
13	3050.0	0.283	-	-	-

Our research analyzed the No. 29 windfarm weather dataset using two algorithms, namely, the DGA and ACO methods. The DGA algorithm was adopted to consider the wake effect problem, and the ACO method was proposed to minimize the cable layout length in the windfarm. The logistic schematic diagram is shown in Figure 4.

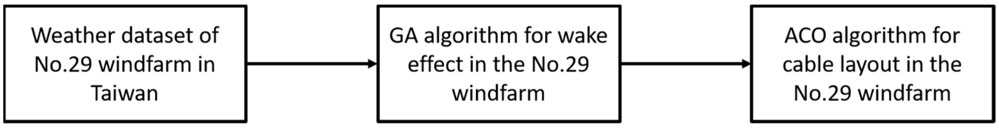

Figure 4. The experimental logistic schematic diagram.

The study analyzed the wake effect variance and cable layout length in the No.29 windfarm based on the 2017–2018 weather dataset provided by SINICA. The major issue is the wake effect influencing the turbine power generation at a low wind velocity state and the associated optimal cable length for turbine connection.

Wake effect:

This study considered the wake effect and used the distributed genetic algorithm to find the optimal layout of the wind. The incoming wind can be separated into the tangentially and normally directed winds between two adjacent turbines. The defining tangential and normal components of the winds are depicted in Figure 5. The tangential component has minimal effect on the turbines. The effective wind velocity is the normally directed wind, and therefore only the wake effect of this component will be included in our current investigation.

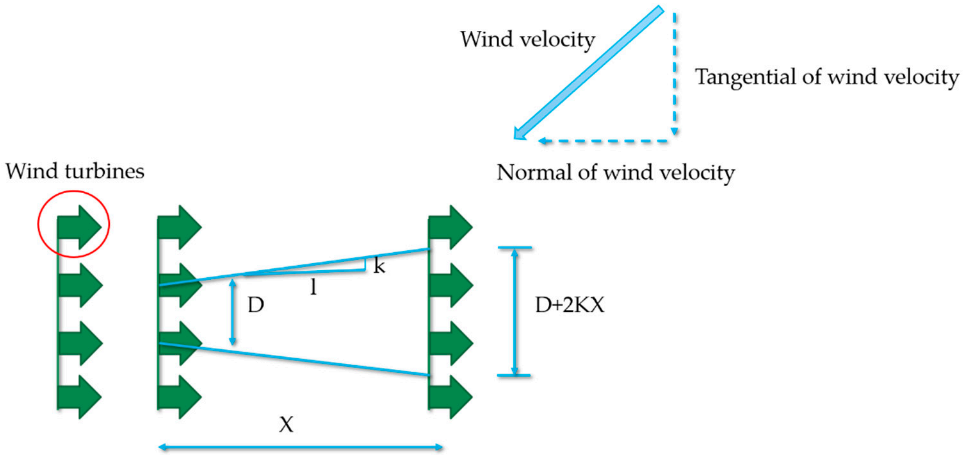

Figure 5. Schematic diagram of the wake effect based on wind direction developed from [11].

The separation of the turbines, X is calculated using Equation (10) as [11]:

$$D + 2 \times k \times C \times X < X \tag{10}$$

where, D is the diameter of the turbine blade;

k is a wake constant (0.04);

C is the width of the entire windfarm.

Based on the above simulation parameters of the wind turbine, after calculation, it was found that when the width of the windfarm was 10 wind turbine distances, the distance between any two adjacent wind turbines, either in the same row or column, needed to be at least 500 m apart.

This study also compared the changes in the overall windfarm efficiency when the distance between two adjacent wind turbines increased from the limiting 500 m to 600 m and 700 m. The results are depicted in Figure 6.

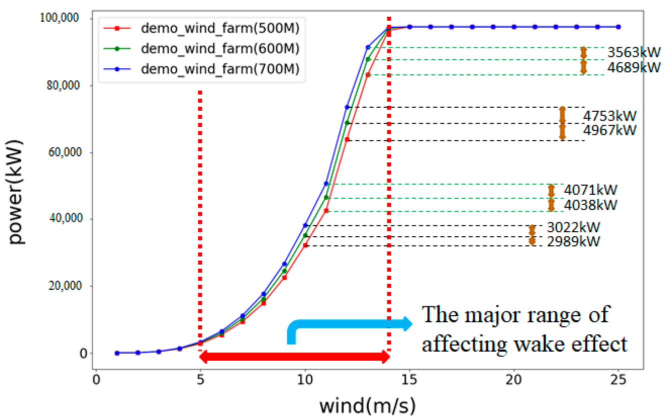

Figure 6. Variation curve of the wake effect caused by different wind velocities and turbines distance.

From the above chart, it can be seen that the overall efficiency of wind power generation has significantly improved by implementing the mitigation measure to counter the wake effect. The effective improvement is especially obvious in the low wind velocity range. For a complete study, it also needs to consider the cable length to minimize operation cost and maximize profits. The length of the power transmission cable will result in more losses and instability. Therefore, this study chose 500 m as the separation between wind turbines to simulate the wind velocity distribution in each windfarm.

Each wind velocity was used for power generation in a demonstration windfarm. In this SINICA dataset study, a demonstration windfarm with a wind turbine setup was introduced, as shown in Figure 7, and the wind velocity distribution was obtained, as shown in Table 3 and Figure 8.

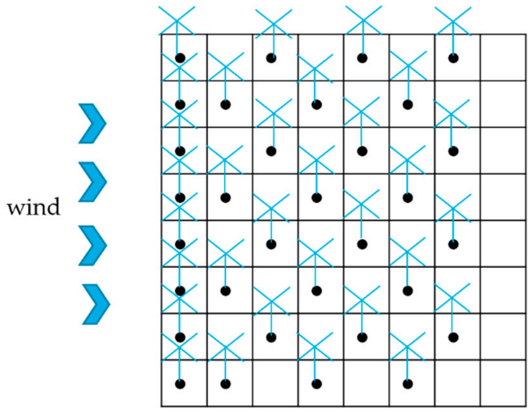

Figure 7. The demonstration windfarm of 32 turbines in 8 × 8 matrix in our real SINICA dataset.

Table 3. Each wind turbine power at demonstration windfarm.

Wind Velocity (m/s)	Power (kW)	Wind Velocity (m/s)	Power (kW)
2	36	14	96,514
3	369	15	97,600
4	1200	16	97,600
5	2764	17	97,600
6	5429	18	97,600
7	9336	19	97,600
8	14,849	20	97,600
9	22,496	21	97,600
10	32,237	22	97,600
11	42,548	23	97,600
12	63,930	24	97,600
13	83,312	25	97,600

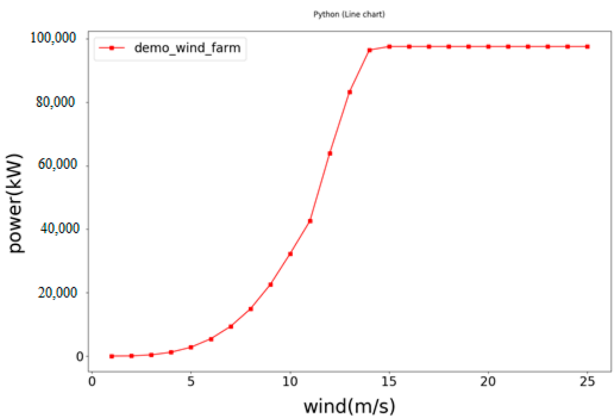

Figure 8. Wind velocity-dependent power output of the demonstration windfarm.

Each wind velocity was applied to optimize wind power generation. In this study, an optimized windfarm was obtained through the distributed genetic algorithm, and the schematic layout is shown in Figure 9. Wind velocity distributions were then considered for the optimized windfarm to evaluate the power generation of each wind velocity, and the results are shown in Table 4 and Figure 10.

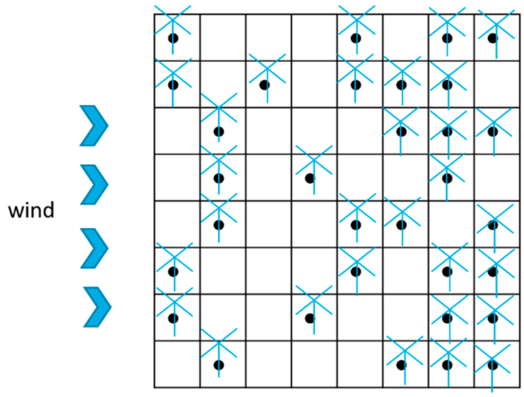

Figure 9. The optimal windfarm layout with our real SINICA dataset (8 × 8 matrix and 32 turbines).

Table 4. Wind power optimization at each wind velocity.

Wind Velocity (m/s)	Power (kW)	Wind Velocity (m/s)	Power (kW)
2	45	14	94,671
3	469	15	97,440
4	1547	16	97,600
5	3508	17	97,600
6	6781	18	97,600
7	11,583	19	97,600
8	18,221	20	97,600
9	27,139	21	97,600
10	38,504	22	97,600
11	50,568	23	97,600
12	68,279	24	97,600
13	84,076	25	97,600

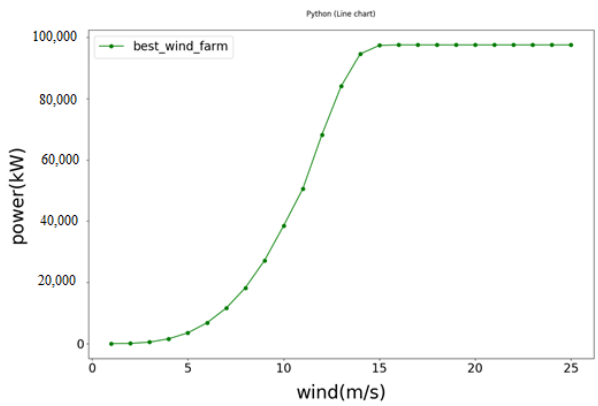

Figure 10. Wind velocity-dependent power output of the optimized windfarm.

The power generation efficiency of the optimized windfarm obtained by the distributed genetic algorithm, which has incorporated mitigation measures to alleviate the wake effect, has shown considerable improvement over that of the conventional demonstration windfarm. The efficiency rating is shown in Figure 11.

In this study, based on the optimized windfarm layout obtained by the distributed genetic algorithm, an optimized windfarm cable layout was also carried out using the ant colony algorithm. The number of ants in the algorithm was 500, the number of iterations was 200. The constraint of the wind cable layout problem is one cable connecting, at most, three turbines. As the total number of turbines was 32 units, which is not divisible by three, the remaining two turbines will simply connect each other. Under the above restriction, the resulting cable length was estimated to be 84,202 m. The schematic layout plan is illustrated in Figure 12. In the figure, we have also schematically included the information of different cable sizes for different power carrying capacities. In Figure 13, we illustrated an actual layout schematic for the optimized windfarm for the planned No. 29 windfarm off the coast of Changhwa, Taiwan.

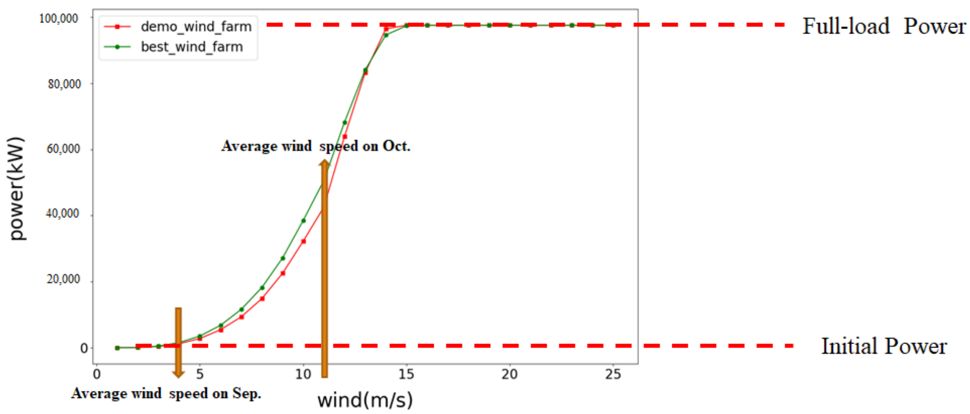

Figure 11. The power comparison of the optimized windfarm and the conventional windfarm.

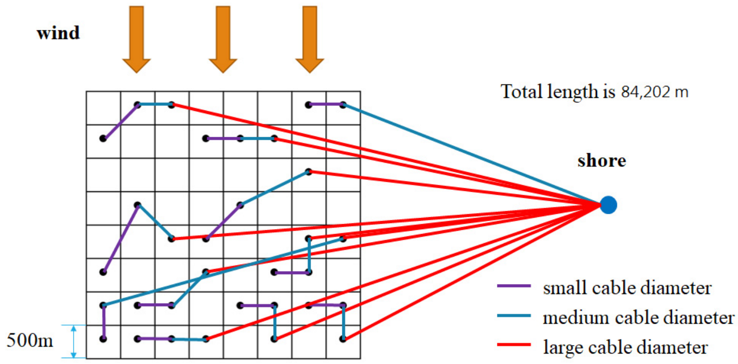

Figure 12. Optimal cable layout by restricting a maximum of three interconnecting turbines.

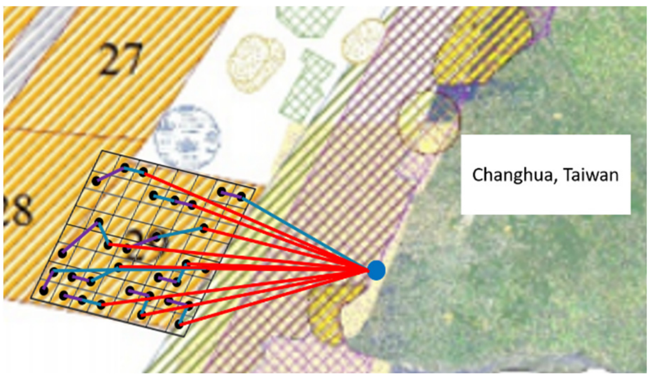

Figure 13. Incorporation of the optimized cable layout onto the map of the planned No. 29 windfarm off the coast of Changhua, Taiwan, to illustrate implementation on an actual site.

A possible second power layout scenario is also proposed by grouping into four substation groups. The major station is associated with four substation groups. Therefore, the second turbine layout constraint is limited to four substation groups. Using this cabling method, the overall cable length is about 46,510 m. The layout for the cabling is depicted in Figure 14.

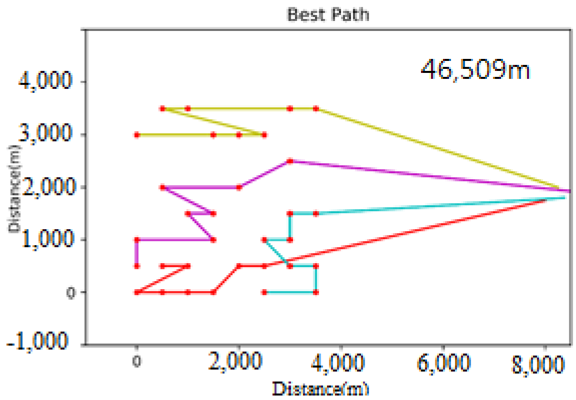

Figure 14. Optimal cable layout by restricting a maximum of 8 interconnecting turbines.

As an alternative for meeting the requirements for different sites, a third power layout scenario is also considered and suggested. The upper limit of the wind turbines was grouped with eight wind turbines connected using radial connection mode. After the algorithm was executed, the system obtained four clusters of wind turbines (each group contained eight wind turbines) and connected the allocated wind turbines to the location of each substation. The substations were located at the four center points of the group, and then these four points were connected to the shore substation terminal. Under this consideration, the resulting cable total length is reduced to 36,620 m, and the layout is schematically illustrated in Figure 15. Even though fewer cables are needed in this scenario, four much larger size cables may be required to connect substations to the shore terminal. The requirement for oversize cables may be undesirable.

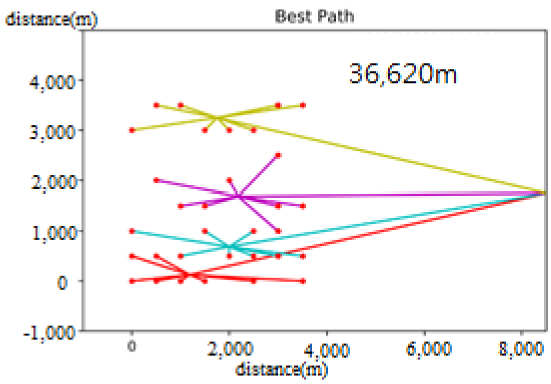

Figure 15. Optimal cable layout using radial connection mode.

The three different cabling plans have their own merits. The main concern is economic, that is, cost minimization. At present, the key issue is the scientific and engineering aspects of the windfarm, and no further in-depth comparison of different cable layout plans will be attempted in the current study.

Wind velocity real data of Academia Sinica:

Based on the windfarm layout calculated by the genetic algorithm, about 3700 pieces of wind velocity data from Academia Sinica were input to calculate the wind velocity and power comparison between the conventional windfarm and the optimized windfarm under the influence of the wake effect, as shown below in Figures 16–19.

As shown in Table 5, our proposed optimized windfarm demonstrated a markedly superior power performance over that of the conventional windfarm under the same wind velocity.

Table 5. Demonstration windfarm and Optimization windfarm power.

Day	4/16	4/17	4/25	5/7	5/8
Optimization (kW)	1,543,801	2,055,285	1,789,095	1,219,146	909,802
Demonstration (kW)	1,295,847	1,901,855	1,546,915	1,018,816	754,267
Difference (kW)	247,954	153,430	242,180	200,330	155,535

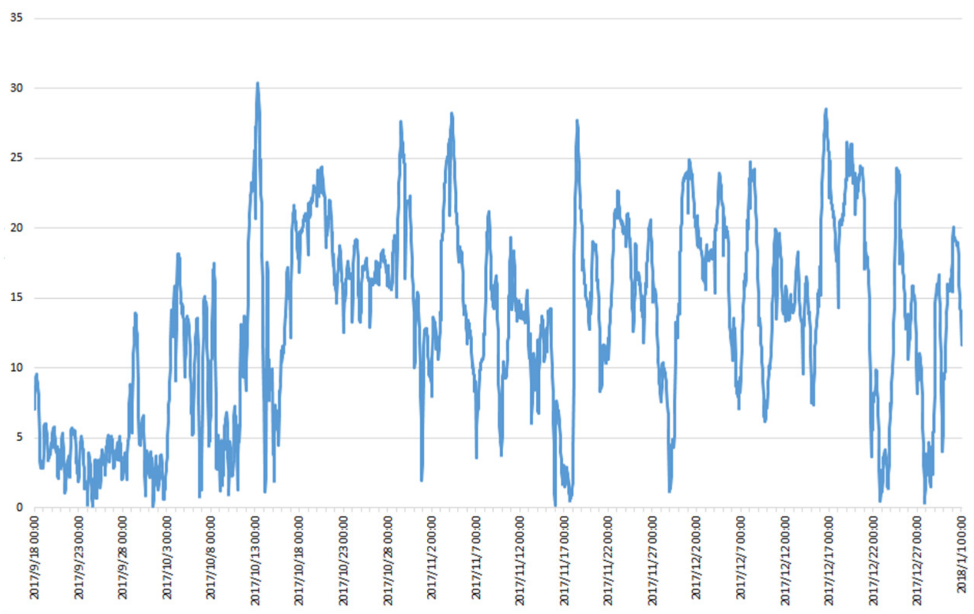

Figure 16. Wind velocity chart between 18 September and 1 January in 2018.

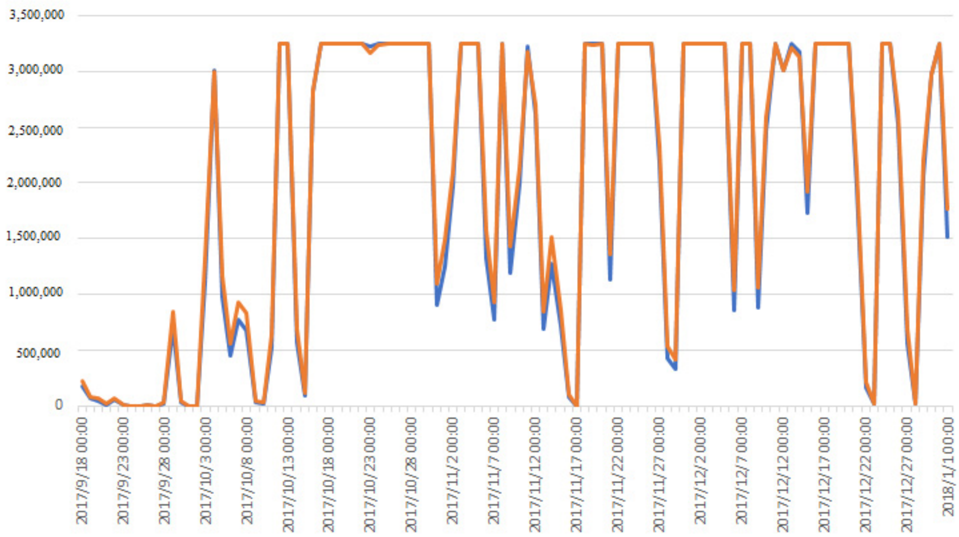

Figure 17. Power chart between 18 September and 1 Januaryin 2018. The orange line is the best power by DGA, and the blue line is the default power.

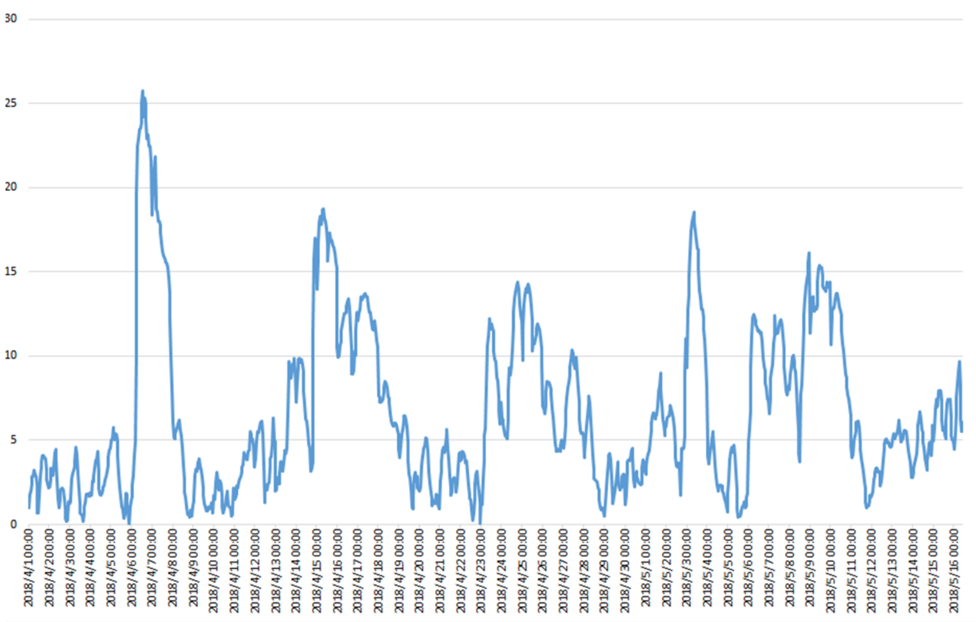

Figure 18. Wind velocity chart between 1 April and 16 May in 2017.

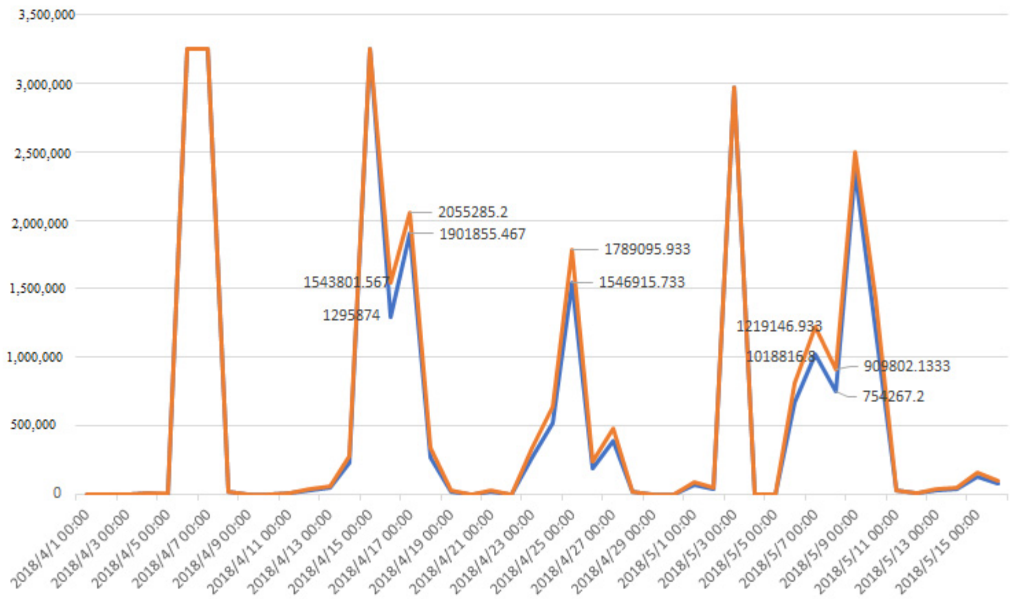

Figure 19. Power chart between 1 April and 16 May in 2017. The orange line is the best power by DGA, and the blue line is the default power.

4. Conclusions

This study considered wake effects, and the case study is based on wind velocity characteristics and an optimization model. The optimized windfarm is constructed by taking into consideration the wake effect and cable layout problem. Through our proposed method, it was found that when the wind velocity was about 5 m/s to 15 m/s, the wake effect and the layout of the windfarm would greatly affect the overall output power of the windfarm. When the wind velocity was lower than 5 m/s, the wind velocity would be too low to drive the turbines. When the wind velocity was greater than 15 m/s, because each turbine and the windfarm as a whole were at full load, the wake effect was not obvious, and no significant difference can be observed. The optimized windfarm obtained by the genetic algorithm of this research showed there was a significant power increase trend in the main affected range.

Actual wind velocity data from Academia Sinica were used to calculate the average daily power of the windfarm. Table 5 shows that the optimized windfarms can generate 15–25 KW more power over that of the conventional windfarm on a daily basis in the period between 4 April and 16 May. The results indicated the need to pay more attention to the importance of the turbine layout in a windfarm.

The optimizing wind turbine layout method was derived by our research, and it was based on turbine number limitations. In order to reduce cable layout costs, the goal for calculating wind cable layouts length is carried out by the ACO algorithm. We design different scenarios according to three practical cable layout cases: 1. One cable connecting a maximum of three turbines; 2. The windfarm is divided into four substation groups with eight turbines per group; 3. The radial connection mode. For the first scenario, our ACO algorithm gives a calculated total length of about 84,202 m, the second scenario the length is about 46,509 m, and the third case yields a total length of 36,620 m. The pros and cons of the three cabling modes may depend on the size of the turbines, which may place a restriction on the size of the cable and also on the actual location of the substation. A comparative study has not been performed at present. In the future, a study will consider these issues with the connection rules adjusted to include the cost and availability of the cables to obtain a complete picture in the assessment of windfarm power efficiency.

Author Contributions: Y.-Z.H., E.-Y.C., S.-W.T. and K.-K.T.; methodology, Y.-Z.H., E.-Y.C., S.-W.T. and K.-K.T.; software, E.-Y.C.; validation, Y.-Z.H.; formal analysis, K.-K.T. and Y.-Z.H.; investigation, Y.-Z.H. and S.-S.L.; resources, Y.-Z.H.; data curation, Y.-Z.H. and E.-Y.C.; writing—original draft preparation, Y.-Z.H. and E.-Y.C.; writing—review and editing, Y.-Z.H. and K.-K.T.; supervision, K.-K.T. and Y.-Z.H.; project administration, K.-K.T.; funding acquisition, K.-K.T., C.-Y.H., S.-C.C., Y.-S.T. and C.-R.C. All authors have read and agreed to the published version of the manuscript.

Funding: This paper was partly supported by Ministry of Science and Technology, Taiwan, under MOST 110-2221-E-019-051-, MOST 109-2622-E-019-010-, MOST 109-2221-E-019-057-, MOST 110-2634-F-019-001-, MOST 110-2634-F-008-005-, MOST 110-2221-E-019-052-MY3, MOST 108-2221-E-019-038-MY2, MOST 110-2634-F-009-018-, National Taiwan Ocean University and China Steel Corporation Grant, and USTP-NTUT-NTOU-109-01, USTP- NTUT-NTOU-108-04.

Acknowledgments: Thanks for Academia Sinica, Taiwan, weather information consultant and Pervasive Artificial Intelligence Research Labs, National Yang Ming Chiao Tung University, Taiwan, support.

Conflicts of Interest: The authors declare no conflict of interest.

References

1. Gu, H. Wake effect in windfarm dynamic modelling. In Proceedings of the 2017 Australasian Universities Power Engineering Conference (AUPEC), Melbourne, Australia, 19–22 November 2017; pp. 1–5.
2. Kusiak, A.; Zheng, H.; Song, Z. Short-Term Prediction of Windfarm Power: A Data Mining Approach. *IEEE Trans. Energy Convers.* **2009**, *24*, 125–136. [CrossRef]
3. Bhardwaj, B.; Jaiharie, J.; Dadhich, R.S.; Ahmed, S.I.; Ganesan, M. Windfarm optimization using Nelder-Mead and Particle Swarm optimization. In Proceedings of the 2021 7th International Conference on Electrical Energy Systems (ICEES), Chennai, India, 11–13 February 2021; pp. 524–529. [CrossRef]
4. Sun, K.; Wang, W.; Qiu, W.; Chen, C.; Zeng, C.; Liu, Y. An Optimal Function-Provided Scheme for Energy Storage System Configured in Windfarm. In Proceedings of the 2020 IEEE 3rd Student Conference on Electrical Machines and Systems (SCEMS), Jinan, China, 4–6 December 2020; pp. 903–907. [CrossRef]
5. Maheri, A.; Jalili, S. A Decision Support System for Decommissioning of Offshore Windfarms: The Data Platform. In Proceedings of the 2021 6th International Symposium on Environment-Friendly Energies and Applications (EFEA), Sofia, Bulgaria, 24–26 March 2021; pp. 1–6. [CrossRef]
6. Lee, D.; Cisek, D.; Yoo, S. Sensor network-based windfarm estimation using deep learning. In Proceedings of the 2017 New York Scientific Data Summit (NYSDS), New York, NY, USA, 6–9 August 2017; pp. 1–3.
7. Tao, Y.; Chen, H.; Qiu, C. Wind power prediction and pattern feature based on deep learning method. In Proceedings of the 2014 IEEE PES Asia-Pacific Power and Energy Engineering Conference (APPEEC), Hong Kong, China, 7–10 December 2014; pp. 1–4.
8. Xiaoyun, Q.; Xiaoning, K.; Chao, Z.; Shuai, J.; Xiuda, M. Short-term prediction of wind power based on deep Long Short-Term Memory. In Proceedings of the 2016 IEEE PES Asia-Pacific Power and Energy Engineering Conference (APPEEC), Xi'an, China, 25–28 October 2016; pp. 1148–1152.

9. Gu, S.; Ji, L. Study on Optimization of Windfarm Micro-Layout. In Proceedings of the 2010 Asia-Pacific Power and Energy Engineering Conference, Chengdu, China, 28–31 March 2010; pp. 1–4.
10. Zhao, M.; Chen, Z.; Hjerrild, J. Analysis of the Behaviour of Genetic Algorithm Applied in Optimization of Electrical System Design for Offshore Windfarms. In Proceedings of the IECON 2006-32nd Annual Conference on IEEE Industrial Electronics, Paris, France, 6–10 November 2006; pp. 2335–2340.
11. Wu, Y.K.; Lee, C.Y.; Chen, C.R.; Hsu, K.W.; Tseng, H.T. Optimization of the Wind Turbine Layout and Transmission System Planning for a Large-Scale Offshore Windfarm by AI Technology. *IEEE Trans. Ind. Appl.* **2014**, *50*, 2071–2080. [CrossRef]
12. Gonzalez, J.S.; Payan, M.B.; Riquelme-Santos, J.M. Optimization of Windfarm Turbine Layout Including Decision Making Under Risk. *IEEE Syst. J.* **2012**, *6*, 94–102. [CrossRef]
13. Huang, H.S. Distributed Genetic Algorithm for Optimization of Windfarm Annual Profits. In Proceedings of the International Conference on Intelligent Systems Applications to Power System, Kaohsiung, Taiwan, 5–8 November 2007; pp. 1–6.
14. Sannino, A.; Breder, H.; Nielsen, E.K. Reliability of Collection Grids for Large Offshore Wind Parks. In Proceedings of the International Conference on Probabilistic Methods Applied to Power Systems, Stockholm, Sweden, 11–15 June 2006; pp. 1–6.
15. Zeng, M.; Huang, L.; Yan, F.; Jiang, D. Notice of Retraction Research of the Problems of Renewable Energy Orderly Combined to the Grid in Smart Grid. In Proceedings of the 2010 Asia-Pacific Power and Energy Engineering Conference, Chengdu, China, 28–31 March 2010; pp. 1–4.
16. Han, X.; Chen, F.; Cui, X.; Li, Y.; Li, X. A power smoothing control strategy and optimized allocation of battery capacity based on hybrid storage energy technology. *Energies* **2012**, *5*, 1593–1612. [CrossRef]
17. Li, X. Fuzzy adaptive Kalman filter for wind power output smoothing with battery energy storage system. *IET Renew. Power Gener.* **2012**, *6*, 340–347. [CrossRef]
18. Jannati, M.; Hosseinian, S.H.; Vahidi, B.; Li, G. Mitigation of windfarm power fluctuation by adaptive linear neuron-based power tracking method with flexible learning rate. *IET Renew. Power Gener.* **2014**, *8*, 659–669. [CrossRef]
19. Katic, I.; Højstrup, J.; Jensen, N. A Simple Model for Cluster Efficiency. *Eur. Wind. Energy Assoc. Conf. Exhib.* **1986**, *1*, 407–410.
20. Available online: https://en.wind-turbine-models.com/turbines/130-enercon-e-101 (accessed on 20 May 2021).